Elsevier Editorial System(tm) for Earth and Planetary Science Letters
Manuscript Draft

Manuscript Number: EPSL-D-15-00041R1

Title: Viscous plugging can enhance and modulate explosivity of strombolian eruptions

Article Type: Letters

Keywords: plugged conduit; eruption dynamics; volcano infrasonic; slug bursting; Taylor bubble; analogue experiments

Corresponding Author: Dr. Elisabetta Del Bello, Ph.D.

Corresponding Author's Institution: Istituto Nazionale di Geofisica e Vulcanologia

First Author: Elisabetta Del Bello, Ph.D.

Order of Authors: Elisabetta Del Bello, Ph.D.; Stephen J Lane, Ph.D.; Mike R James, Ph.D.; Edward W Llewellin, Ph.D.; Jacopo Taddeucci, Ph.D.; Piergiorgio Scarlato; Antonio Capponi

Abstract: Strombolian activity is common in low-viscosity volcanism. It is characterized by quasi-periodic, short-lived explosions, which, whilst typically weak, may vary greatly in magnitude. The current paradigm for a strombolian volcanic eruption postulates a large gas bubble (slug) bursting explosively after ascending a conduit filled with low-viscosity magma. However, recent studies of pyroclast textures suggest the formation of a region of cooler, degassed, more-viscous magma at the top of the conduit is a common feature of strombolian eruptions. Following the hypothesis that such a rheological impedance could act as a 'viscous plug', which modifies and complicates gas escape processes, we conduct the first experimental investigation of this scenario. We find that: 1) the presence of a viscous plug enhances slug burst vigour; 2) experiments that include a viscous plug reproduce, and offer an explanation for, key phenomena observed in natural strombolian eruptions. Our scaled analogue experiments show that, as the gas slug expands on ascent, it forces the underlying low-viscosity liquid into the plug, creating a low-viscosity channel within a high-viscosity annulus. The slug's diameter and ascent rate change as it enters the channel, generating instabilities and increasing slug overpressure. When the slug reaches the surface, a more energetic burst process is observed than would be the case for a slug rising through the low-viscosity liquid alone. Fluid-dynamic instabilities cause low and high viscosity magma analogues to intermingle, and cause the burst to become pulsatory. The observed phenomena are reproduced by numerical fluid dynamic simulations at the volcanic scale, and provide a plausible explanation for pulsations, and the ejection of mingled pyroclasts, observed at Stromboli and elsewhere.

Viscous plugging can enhance and modulate explosivity of strombolian eruptions

E. Del Bello[1], S.J. Lane[2], M.R. James[2], E.W. Llewellin[3], J. Taddeucci[1], P. Scarlato[1], Capponi, A. [2]

[1] *Istituto Nazionale di Geofisica e Vulcanologia, Via di Vigna Murata 605, 00143, Rome, Italy*

[2] *Lancaster Environment Centre, Lancaster University, Lancaster LA1 4YQ, UK*

[3] *Department of Earth Sciences, Durham University, South Road, Durham DH1 3LE, UK*

Corresponding author: Elisabetta Del Bello, Istituto Nazionale di Geofisica e Vulcanologia, Via di Vigna Murata 605, 00143, Rome, Italy, +39-0651860744, elisabetta.delbello@ingv.it

HIGHLIGHTS

- We present laboratory experiments in which gas slugs ascend a pipe plugged with a viscous liquid
- The presence of a viscous plug enhances burst vigour
- Slug–plug interaction causes pulsatory bursting resembling natural strombolian eruptions
- Experiments indicate slug passage promotes mingling between vertically stratified magmas

ABSTRACT

Strombolian activity is common in low-viscosity volcanism. It is characterized by quasi-periodic, short-lived explosions, which, whilst typically weak, may vary greatly in magnitude. The current paradigm for a strombolian volcanic eruption postulates a large gas bubble (slug) bursting explosively after ascending a conduit filled with low-viscosity magma. However, recent studies of pyroclast textures suggest the formation of a region of cooler, degassed, more-viscous magma at the top of the conduit is a common feature of strombolian eruptions. Following the hypothesis that such a rheological impedance could act as a 'viscous plug', which modifies and complicates gas escape processes, we conduct the first experimental investigation of this scenario. We find that: 1) the presence of a viscous plug enhances slug burst vigour; 2) experiments that include a viscous plug reproduce, and offer an explanation for, key phenomena observed in natural strombolian eruptions. Our scaled analogue experiments show that, as the gas slug expands on ascent, it forces the underlying low-viscosity liquid into the plug, creating a low-viscosity channel within a high-viscosity annulus. The slug's diameter and ascent rate change as it enters the channel, generating instabilities and increasing slug overpressure. When the slug reaches the surface, a more energetic burst process is observed than would be the case for a slug rising through the low-viscosity liquid alone. Fluid-dynamic instabilities cause low and high viscosity magma analogues to intermingle, and cause the burst to become pulsatory. The observed phenomena are reproduced by numerical fluid dynamic simulations at the volcanic scale, and provide a plausible explanation for pulsations, and the ejection of mingled pyroclasts, observed at Stromboli and elsewhere.

KEYWORDS

plugged conduit; eruption dynamics; volcano infrasonic; slug bursting; Taylor bubble; analogue experiments

1. INTRODUCTION

Strombolian activity may be very long-lived, with episodes lasting years, decades, or even centuries. This longevity, coupled with the photogenic nature of the explosions, has made some persistently active strombolian volcanoes popular tourist destinations – for instance, more than ten thousand tourists visit the summit of Stromboli itself each year. Although usually benign, strombolian activity spans a range of magnitudes, and includes events that are much more violently explosive and may pose a significant hazard to tourists and nearby communities. It is important, therefore, to determine the factors that cause a usually mildly explosive system to generate more violent explosions.

The discrete explosions that characterize the strombolian eruptive style are interpreted as the impulsive bursting of over-pressured gas pockets – or slugs – at the top of a magma column (Chouet et al., 1974; Blackburn et al., 1976, Burton et al., 2007). Overpressure is a fundamental consequence of large gas bubbles rising from depth and expanding against viscous and inertial retardation as pressure decreases (James et al., 2008; 2009; Del Bello et al., 2012). This behaviour is generally restricted to basaltic or andesitic magmas, because these systems have sufficiently low viscosities to allow bubble coalescence and decoupling of gas slugs from magma over short time scales (order of seconds to hours). Experimental and numerical models within the volcanological literature consider the slug rising through a medium with uniform viscosity and density. These models provide first order explanations of the dynamics of gas expansion, overpressure, and generation of seismic and acoustic signals (e.g., Vergniolle and Brandeis, 1996; Vergniolle et al., 1996; Seyfried and Freundt, 2000; Parfitt, 2004; O'Brien and Bean, 2008; D'Auria and Martini, 2009; James et al., 2009; Kobayashi et al., 2010; Del Bello et al. 2012; Gerst et al., 2013; Kremers et al., 2013; Nguyen et al., 2013; Lane et al. 2013, Sánchez et al., 2014). However, none of these approaches encompasses the presence of a region of degassed, crystalline magma with increased viscosity and strength in the shallow conduit. Such a rheological impedance – which can be termed a 'plug' – is commonly inferred, and physically plausible, at active strombolian-type vents (e.g., Gurioli et al., 2014).

Textural data from many strombolian-type volcanoes support the coexistence of magmas that have contrasting rheology as a result of cooling- and degassing-driven crystallisation (e.g, Taddeucci et al., 2004, Cimarelli et al., 2010; Kremers et al., 2012; Ruth and Calder, 2013). Considering Stromboli as a canonical case during its 'normal' activity, it is very common to find both bubble-rich, crystal-poor textures and bubble-poor, crystal-rich textures

intermingled within a single pyroclast (e.g., Lautze and Houghton, 2005; 2007; Polacci et al., 2006, 2009; Colò et al., 2010; D'Oriano et al., 2011, Gurioli et al., 2014). It has been proposed that these textures represent mingling of relatively fresh, gas-rich magma with older, completely or partially degassed magma, in the shallow conduit (e.g., Lautze and Houghton, 2005). Cooling, degassing and associated crystallization of the magma in the upper conduit cause it to have a much higher viscosity then its deeper, fresh counterpart. This rheological distinction is not to be confused with the so called 'high porphiricity' (HP or '*black*') and 'low porphiricity' (LP or '*golden'*) magma types (e.g., Métrich et al., 2005); these are distinguished on the basis of geochemical and isotopic analyses, with LP magma thought to occupy the system at depths greater than ~3.5 km. At the volcanic scale, rapid expansion of the gas slug associated with the burst process occurs only within the last few tens of meters of the magma column (James et al., 2008). Hence, the region of plug–slug interaction is limited to the shallowest portion of the conduit, entirely within the HP magma domain.

The presence of a plug, and its thickness, must have an important impact on eruption dynamics. For instance, we would expect the viscous plug to retard slug expansion, thereby promoting the development of overpressure within the slug as it rises. We would also expect the plug material and thickness to affect the dynamics of the bursting process. Lautze and Houghton (2007) were the first to suggest that changing proportions of magma with differing viscosities influenced eruption frequency and vigour supporting the notion that plug thickness could change over time. These factors introduce additional complexity compared with the unplugged scenario (e.g., Andronico et al. 2008). This complexity might be manifest in the seismo-acoustic signatures of the explosions (e.g., Johnson and Lees, 2000, Lyons et al., 2012), and in the visual character of the explosions. We note, for instance, that recent high-speed videography studies have identified that gas escape during strombolian explosions is typically pulsatory (Taddeucci et al., 2012, Gaudin et al., 2014), suggesting greater complexity than simple bursting of an overpressured slug. Understanding the role that a viscous plug plays in modulating the dynamics of slug ascent and burst is, therefore, of considerable importance in the interpretation of the waveform and amplitude of generated pressure changes (Lane et al., 2013). In order to gain insight into the complex volcanic system (e.g., Gurioli et al., 2014), we use first-order laboratory experiments to evaluate the influence of a Newtonian, high-viscosity plug on gas slug ascent and burst in a vertical tube. Our experiments build on previous work carried out in single-viscosity systems (James et al., 2004; 2006; 2008; 2009; Lane et al., 2013), and we adopt a similar analogue methodology. We also use a computational fluid dynamic model (James et al., 2008; Chouet et al., 2010) to conduct numerical

simulations of the same scenario at the volcano scale, in order to explore the applicability of our laboratory results to the natural system.

2. EXPERIMENTAL METHOD

2.1. Scaling considerations

We model an idealised volcanic scenario in which a layer of high-viscosity magma of variable thickness overlies a column of low-viscosity magma. The behaviour of a slug ascending a vertical pipe filled with a viscous liquid may be described via a number of dimensionless groups, namely the Morton number *Mo*; the Eötvös number *Eo*; the inverse viscosity N_f; the Froude number *Fr*; and the Reynolds number *Re* (e.g, Viana et al. 2003, Llewellin et al., 2012). These groups are defined and calculated for the volcanic and experimental scenarios in the Supplementary Content. We show that, in both systems, surface tension plays a negligible role in slug ascent (e.g, Seyfried and Freund, 2000) hence behaviour is controlled by the inverse viscosity N_f,

$$N_f = \frac{\rho}{\mu}\sqrt{gD^3}, \qquad (1)$$

where ρ and μ are the density and dynamic viscosity of the liquid, g is the gravitational acceleration, and D is the tube diameter.

For a canonical representation of parameters at volcano-scale, we choose a viscosity of 5×10^4 Pa s for the plug based on recent estimations for magma in the shallowest part of Stromboli's conduit (e.g., Gurioli et al. 2014) and 50 Pa s for the underlying magma based on minimum accepted values for basaltic melts (Table 1). Although density differences are observed among pyroclasts that tap the uppermost conduit (e.g., Lautze and Houghton, 2005), we exclude density stratification from our analysis and assume that the volcanic system is dynamically stable (or that gravitational instability develops on timescales much longer than that needed for plug formation). Based on values in Table 5 of Gurioli et al. (2014), we estimate a density of approximately 1000 kg m^{-3} for the plug and underlying magma during the active flow process. The respective values of the inverse viscosity in the plug and underlying magma in a 5-m-diameter conduit are then $N_f \approx 0.7$ and $N_f \approx 700$ putting slug behaviour in the viscous and inertial regimes respectively (e.g., White and Beardmore, 1962). The dimensionless thickness (λ') of the falling film of magma around the rising slug is essentially independent of N_f in these regimes (Llewellin et al., 2012), with values of 0.33 and 0.14 respectively. We also calculate the fraction of the tube cross-section occupied by the falling film $A' \approx 0.55$ if magma viscosity is that of the plug, and $A' \approx 0.25$ if viscosity is that of the underlying magma (see Supplementary Content for derivation). Consequently, a gas slug is predicted to narrow

substantially when entering the plug zone (occupying ~60% of the cross sectional area it occupies in the underlying liquid).

In the laboratory we use castor oil (viscosity 0.986 Pa s; density 970 kg/m^3) and water (viscosity 0.001 Pa s; density 1000 kg/m^3) as respective analogues for the plug and underlying magma (see Table 1). Given a pipe diameter of 2.5 cm, this gives us values of $N_f \approx 12$ and $N_f \approx 12{,}000$ in the plug and underlying liquid respectively. Although these values are somewhat higher than their counterparts in the volcanic system (i.e., the experiments are relatively less viscous), they lie in the same viscous and inertial regimes respectively; the divide between the regimes was found to be around $N_f \approx 100$ by Llewellin et al. (2012). Consequently, the fractions of the pipe cross-section occupied by a falling film of oil or water ($A' \approx 0.53$ and $A' \approx 0.16$ respectively) are similar to those in the volcanic scenario. The experimental N_f values also lie in the same regions where λ' is almost constant, and the viscosity ratio is of order 1000 for both experimental and volcanic scenarios.

2.2. Experimental apparatus

The experimental apparatus (Fig. 1) comprises a vertical glass tube 0.025 ± 0.001 m in diameter (D), filled with liquid to a height of 1.80 ± 0.01 m, and with a nominal ambient pressure above the liquid P_a of 3.0 ± 0.1 kPa to scale for gas expansion during ascent (James et al. 2008). Experiments were carried out by injecting a known volume of air (V_0) equilibrated to the same pressure as the base of the tube. Slug rising and bursting were filmed at 299.7 ± 0.1 frames per second with a Casio Exilim FX1 camera. Pressure in the air above the liquid (P_A) was measured at 1 kHz (NI PCI 6034E data-logger, with 16 channels) with two Honeywell differential 163PC01D75 transducers, and within the liquid at the base of the tube (P_L,) with one BOC Edwards A.S.G. 1000 sensor. Pressure variation (ΔP_A and ΔP_L) is then obtained by subtracting measured pre-injection values from the recorded pressure. To reduce noise, ΔP_A is smoothed by taking the mean of the two transducers and a 5-point running average, and ΔP_L is smoothed with a varying running average corresponding to the apparatus resonant 'bounce' frequency (James et al., 2008).

Air volumes (V_0) of 2, 4, 6, 8 and 10 ± 0.1 ml were injected into a water column (single-liquid 'control' experiments) or into a water column whose top was replaced with a layer of castor oil of thickness h equal to either 2D (i.e., h = 0.05 m of oil above 1.75 m of water), or 7D (h = 0.18 m of oil above 1.62 m of water). Each experiment was repeated to assess both reproducibility and variability under nominally identical conditions. The

injected volumes non-dimensionalize to give $V_a' = 0.09$, 0.18, 0.28, 0.37 and 0.45 respectively (Del Bello et al., 2012; see Supplementary Content for methodology). For the volcanic system, these experiments represent erupted gas volumes of 7 – 37 m^3 (1.2 to 6 kg) and plugs 0, ~ 10, and ~ 35 m thick (video V01). In both systems, V_a' is calculated based on the properties of the liquid underlying the plug, and in a single liquid system would result in passive expansion with slug overpressure only becoming significant at the largest bubble size (Lane et al., 2013).

3. EXPERIMENTAL RESULTS

3.1. Control experiments without viscous plug

The injected air forms a slug that ascends and expands within the tube, surrounded by a falling film of water that shows no discernible ripples (Fig. 2a, video V01). As noted in previous experimental studies, base pressure ΔP_L decreases during slug ascent (Fig. 3a), because an increasing water mass in the falling film is dynamically supported on the tube wall (e.g., James et al., 2004). Slug expansion, which accelerates during ascent, displaces the liquid's free surface upwards. The slug bursts when its nose catches the liquid surface. After burst, the water film drains back, developing ripple structures, and ΔP_L increases to the pre-injection value.

Acceleration of the liquid's free surface and air liberation during the burst process generate a reproducible pulse (Fig. 3a) in the pressure above the liquid ΔP_A (Lighthill, 1978). The resulting waveforms are similar to those observed in experiments conducted with oil ~100 times more viscous than water (Lane et al., 2013) indicating insensitivity to absolute viscosity under inertial conditions. The peak excess pressure $\Delta P^{\wedge}_A$ scales linearly with dimensionless slug volume (Fig. 4) as also observed by Lane et al. (2013).

3.2. Thin viscous plug experiments

The presence of a thin viscous plug (plug thickness h = 2D) slightly retards slug expansion during ascent. A smaller initial decrease in ΔP_L compared with the control experiments, or even a slight ΔP_L increase for the smallest V_0, was observed (Fig. 3b). Slug expansion drives an intrusion of water into and through the plug (Fig. 2b, Video V02). The intruding water core displaces and spreads oil along the tube wall to form a high-viscosity annulus, longer than the initial plug, enclosing a low-viscosity channel of water. The radial thickness of the oil annulus averages ~3 mm, and increases slightly from bottom to top, forming a dynamic, partial constriction of the effective tube cross-section. Once the water core breaches the plug, extruded water accumulates above it, the accumulated volume increasing as the slug expands.

When the slug reaches the base of the annulus, it exploits the low-viscosity pathway provided by the water core to ascend through it. A three-layer, axi-symmetric flow configuration is formed, with the ascending slug surrounded by a falling film of water, all enclosed within the oil annulus, which appears to be stationary (Fig. 2b) on this time-scale. As the slug rises through the annulus, ΔP_L rapidly decreases by a factor of 2 to 4 compared with the control experiment (Fig. 3b). As the slug encounters the dynamic geometry change created by the high-viscosity annulus, instabilities form in the falling water film below the annulus. We suggest this could be caused by a reduction in the flux of water into the falling film below the annulus caused by the narrowing of the ascending slug within the annulus. As the slug ascends through, and emerges from the high-viscosity annulus, further instabilities begin to develop within the annulus. These are caused by the emergence of the slug from the dynamic geometry of the annulus (James et al., 2006) and the rapid waning of the flow processes that generated both the falling water film and the oil annulus. As both liquids drain back after burst and ΔP_L increases to the pre-injection value large downward ripples develop along the pipe walls (Fig. 2b). The ripples induce ΔP_L fluctuations 5 to 10 times larger than observed in the control experiments (Fig. 3b).

$\Delta P^{\wedge}_A$ is slightly greater than in the control experiments (Fig. 4). The ΔP_A waveform has a similar initial pulse, but lasts longer and becomes more complex and variable (Fig. 3b). The video (V02) suggests ripples in the draining liquids cause significant and variable impedance of air escape rate from the slug, modulating ΔP_A.

3.3 Thick viscous plug experiments

A thick viscous plug (plug thickness $h = 7D$) retards slug expansion during ascent more strongly than a thin one, producing a higher maximum ΔP_L (Fig. 3c, maximum ΔP_L for the 2 ml slug is out of figure to the left). Small and large slugs display contrasting behaviour. The 2 ml slugs expand modestly, intrude minimal water into the oil, and are fully accommodated in the oil plug (Fig. 2c), passing slowly through it without developing any instability. Bursting is visible as a rupturing of an oil meniscus (Video V03), concomitant with a minimum in ΔP_L (Fig. 2c). Negligible acceleration of the free surface is observed and no ΔP_A signal is detected. This rupture dynamics is typical of the ‘quiescent’ regime experimentally identified by Lane et al. (2013), and is analogous to the bursting process observed by Kobayashi et al. (2010).

Expansion of the 4-8 ml slugs intrudes water significantly into the plug, with instabilities within the falling water film observed below the annulus as the slug ascends. Only the 10 ml slugs intrude sufficient water to accumulate it atop the oil annulus (Fig. 2d, Video V04). In this case, rapid slug expansion through the long, narrow, water-filled

annulus causes a dramatic ΔP_L drop, as the entire plug mass becomes dynamically supported by the tube wall (Fig. 3c). The rapid change in flow structure caused by slug expansion strongly destabilizes the annulus causing its upper reaches to disrupt into mixed water/oil globs. The bursting process is complex, involving transient restriction and blockage of the tube by the collapsing annulus and draining water (Fig. 2d). At burst, the slug base is still below the base of the annulus, leaving it fully supported by the tube wall. As the slumping annulus, mixed with water, encounters the water surface at the slug base, a reproducible step increase in ΔP_L occurs (Fig. 3c), unique for the 10 ml slug.

A thick high-viscosity plug increases $\Delta P^{\wedge}_A$ by a factor of ~ 3 to 5 compared with the control (Fig. 4). ΔP_A waveforms also become more complex as V_0 increases (Fig. 3c), with: a) negligible signal at 2 ml; b) some similarity to control experiments at 4-8 ml; and c) large secondary peaks at 10 ml, some of them appearing up to 0.5 s after the primary peak. The ΔP_A peaks at 0.23, 0.27, and 0.47 s in Fig. 3c represent secondary pulses of air escaping temporary blockages of the tube caused by unstable slumping oil and globs of oil descending after being previously ejected upward. These peaks are observed in each 10 ml run, but their timing varies.

4. THE IMPACT OF VISCOUS PLUGGING ON SLUG BURST DYNAMICS

Our experimental results demonstrate that the presence of a viscous plug impacts strongly on slug ascent and burst. The viscous plug retards slug growth during ascent, implying an increase in slug overpressure (Bagdassarov, 1994), which drives more vigorous bursting. Slug expansion during ascent causes the underlying liquid to penetrate the viscous plug, creating an annular constriction through which the slug must pass. The annulus increases the fraction of the pipe cross-section occupied by the liquid, creating a dynamic narrowing in the conduit geometry. The area occupied by the slug reduces by nearly half when entering the annulus, decreasing from 0.84 to 0.47 of the pipe cross section. The slug expansion rapidly accelerates as it passes through the constriction as a result of this decrease in its cross-sectional area. Increasing slug expansion enhances free surface acceleration, causing excess pressure $\Delta P^{\wedge}_A$ to increase accordingly (Lighthill, 1978). Plotting $d(\Delta P_A)/dt$, representing synthetic infrasonic waveforms resulting from the experimental fluid-dynamic source mechanism (Lane et al.,2013), also illustrates positive correlation of the main peaks with h and V_0, and also shows that secondary oscillation pulses are more prominent when the viscous plug is present (Figure 5). The two-layer liquid flow, generated by slow intrusion of water into and through the oil plug as the ascending gas slug expands, becomes dynamically unstable on rapid change to a three-layer fluid flow as the gas slug expands through the water core. The resulting instabilities cause transient

blocking of the slug's narrow path, adding significant complexity to the burst process. As a result, the slug pinches into shorter gas pockets, causing pulsatory bursting that modulates the associated ΔP_A signal after the main pulse. Finally, the fluid-dynamic instabilities cause the two liquids to inter-mingle; this effect is strongest when a large slug ascends through a thick viscous plug.

5. VOLCANO-SCALE SIMULATION

A three-dimensional numerical simulation of the final ascent stage of a slug of gas at volcano scale (as in James et al., 2008; Chouet et al., 2010) was carried out using the FLOW-3D fluid dynamics simulation package (video V05). The simulation was performed with a conduit diameter of 3 m, a plug thickness h = 2D (~6 m), an underlying magma thickness of 194 m (simulating a total 200 m thick magma column), viscosities of 20,000 and 20 Pa, respectively, and a non-dimensional slug volume V_a' = 0.28 (equivalent to ~ 22 m^3 of gas). This gave N_f values of ~ 0.8 and ~ 800 for the viscous plug and the underlying magma respectively. Although slightly lower than the 'canonical' volcanic system, these N_f values represent the minimum acceptable values for basaltic melts (e.g. Vergniolle and Jaupart, 1986); these were the highest values we could use without encountering numerical instabilities.

The CFD simulation shows a phenomenology similar to that observed experimentally (Figure 6). Low viscosity liquid intrudes into and above the high viscosity plug, causing it to form an annulus as the gas bubble expands on ascent (Figure 6a, b); gas follows the low viscosity intrusion through the high viscosity annulus, with the slug narrowing in the annulus and 'ponding' below the annulus (Figure 6c). Ripples of instability form within the falling film below the annulus, and collapse of the low viscosity liquid above the annulus segments the ascending slug (Figure 6d). This detailed level of similarity between our scaled experiment and the modelled volcanic scenario provides resilience in applying the observed phenomena to the natural volcanic case.

6. IMPLICATIONS FOR STROMBOLIAN VOLCANIC ERUPTIONS

Our laboratory experiments allow us to develop a general conceptual model for slug ascent and burst through a viscous plug (Fig 7) that could give insight into key phenomena observed in natural strombolian eruptions. Firstly, several authors have described the simultaneous eruption, during a single strombolian explosion, of pyroclasts from magmas with contrasting textural and rheological properties, sometimes mingled within a single pyroclast (e.g.,Taddeucci et al., 2004; Lautze and Houghton, 2005; 2007; Gurioli et al., 2014). Our experiments open a new possible scenario, in which mingling results from the fluid dynamic instabilities that develop when a slug expands

through the self-organizing geometry of a core of low-viscosity magma within an annular plug of high-viscosity magma. The instabilities cause the two magmas to mingle in the slug burst region, scavenging both into pyroclasts.

Secondly, high-speed videography has revealed the presence of ejection pulses – highly variable in duration and pyroclast velocity – within individual strombolian explosions (Taddeucci et al., 2012). Experimentally, these pulses are caused by transient blocking of the conduit by the same instabilities, supporting the hypothesis, proposed by Taddeucci et al. (2012), that "transient gas pockets formed by the repeated collapse of the liquid film lining conduit walls during the bursting of long slugs". We observe a semi-quantitative similarity between pyroclast ejection velocity at Stromboli and air pressure in the scaled experiments. The experimental timescale of the individual pressure pulses (~ 0.05 s) is about a factor of ten shorter than the duration of the whole bursting process (~ 0.5 s), matching well the scaling factor for the timescale of ejection pulses (~0.1-1 s) to that of strombolian explosions (a few seconds to tens of seconds).

Our experimental findings provide a new reference for understanding, interpreting, and modelling strombolian volcanic eruptions. The instabilities that cause pulsations in the eruption are only observed in experiments that include a viscous plug (compare control experiments and previous studies, e.g., James et al., 2009; Lane et al., 2013), suggesting that the presence of a plug could be a plausible pre-requisite for the generation of complex multi-pulse behaviour, as may be observed from infrasound and videography. Furthermore, the formation of an annulus of higher-viscosity magma in our experiments advocates the existence of a 'dynamic' conduit geometry, which changes cyclically in response to the passage of slugs. The balance of timescales of plug-forming and plug-consuming processes (i.e, magma degassing, cooling, crystallization, and entrainment of fall-back material, vs. the return time and volume of passing slugs) will create a complex feedback controlling the generation and recovery of the dynamic and effective conduit geometry (James et al., 2006), explosion dynamics, and the linked frequency and intensity of explosions.

Finally, our results indicate that the increase in explosivity and complexity of strombolian eruptions related to the presence of a viscous plug are mirrored by differences in the first time derivative of pressure variation $d(\Delta P_A)/dt$, i.e., atmospheric infrasound. In our experiments, a 'thick' plug increases peak pressure of the main 'burst' by a factor of 3 to 5 compared with no plug, and is associated with the development of more prominent secondary peaks. Extrapolating the observed trends in natural volcanic eruptions requires care and is beyond the intention of

this work. However, a quick by-eye comparison with infrasonic signals generated by eruptions from the 'Hornito' 2012 vent at Stromboli (Figure 6E in McGreger and Lees, 2004, shows remarkable similarity to the $d(\Delta P_A)/dt$ synthetic waveform from the 10-ml, 7D experiment (Figure 8). Qualitatively the first pulse is well matched, in similarity to single viscosity systems (Lane et al., 2013); however, in contrast to the single viscosity system, the subsequent secondary oscillations are also well matched, suggesting that slug interaction with a thick viscous plug could provide a plausible first-order mechanism for such infrasonic signals. Thus, we expect that, during volcanic eruptions, the presence and thickness of a viscous plug introduces another degree of freedom to the system, which may act to increase variability and reduce the certainty of interpretation of air and ground motion signals. This ultimately bears on the importance of multiple monitoring, during eruptions, of parameters such as erupted gas masses, and magma rheology, for a more accurate interpretation of infrasonic signals.

7. CONCLUSIONS

The presence of a viscous plug at the top of a volcanic conduit can play a major role in modifying the nature of strombolian explosions. A viscous plug increases the explosivity of strombolian eruptions by enhancing slug overpressure. The plug introduces complexities by modulating the slug expansion and burst process, explaining observed eruption pulses and secondary acoustic signals. The presence of a plug also explains the commonly observed eruption of mingled-texture pyroclasts.. The key fluid-dynamic mechanism is the expansion of the ascending gas slug driving intrusion of low viscosity magma into the overlying plug. The resulting annulus of plug material surrounds an intrusion of low-viscosity magma through which the slug then rises to the free surface. The 'rapid' expansion of the gas slug through the low-viscosity intrusion destabilises the liquid annulus, which acts as a dynamic constriction of the conduit, modulating gas escape and strongly affecting the geophysical signals, such as infrasound, associated with the expansion and burst of the slug. For the same gas volume, a viscous plug leads to the generation of different types of pressure signals. Thus, our experimental results reveal some important aspects of the explosivity of basaltic systems. In particular, they evidence that besides gas volume, the presence and extent of viscous plugging must be considered for the interpretation of infrasonic measurements of strombolian eruptions. In this study, viscous plugs are modelled as discrete bodies, whereas in real volcanic systems, plugs are likely to be gradational features. Despite continuous monitoring of Stromboli volcano these features are still not predictable or fully understood. Further work is required to determine the impact that this has on our first order findings.

VIDEO DESCRIPTION

Videos V01, V02, V03, and V04 contain video sequences and synchronised pressure variations acquired during the following experiments: V01) control experiment (no viscous cap, $h = 0D$), 4 ml slug; V02) thin viscous cap ($h = 2D$), 4 ml slug; V03) thick viscous cap ($h = 7D$), 2 ml slug; V04) thick viscous cap ($h = 7D$), 10 ml slug. Unfiltered and filtered pressure variations are reported for both ΔP_A (pink and red lines, respectively) and ΔP_L (grey and black lines). Predicted atmospheric acoustic pressure (yellow line, $d\Delta P_A/dt$) is also reported for the three experiments in the movies that show P_A signals. Video V05 contain the result of the CFD simulation at the volcanic scale ($V_0 = 22$ m^3, $P_a = 10^5$ Pa, $\mu_1 = 20$ Pas, $\mu_2 = 20000$ Pas; h =6 m, D = 3 m, magma column height 200 m) described in section 5.

ACKNOWLEDGEMENTS

This work was partly supported by ED Ph.D. project grant (University of Bologna) funded by INGV. A.C. received funding from the People Programme (Marie Curie Actions) of the European Union's Seventh Framework Programme (FP7/2007-2013) under the project NEMOH, REA grant agreement n° 289976. We thank Sylvie Vergniolle and an anonymous reviewer for their constructive comments, which helped improve the manuscript. We also thank Tamsin Mather for her editorial handling of the manuscript.

REFERENCES CITED

Andronico, D., Corsaro, R.A., Cristaldi, A., Polacci, M., 2008. Characterizing high energy explosive eruptions at Stromboli volcano using multidisciplinary data: An example from the 9 January 2005 explosion. J. Volcanol. Geotherm. Res. 176, 541–550.

Bagdassarov, N.S., 1994. Pressure and volume changes in magmatic systems due to the vertical displacement of compressible materials. J. Volcanol. Geotherm. Res. 63, 95–100.

Blackburn, E.A., Wilson, L., Sparks, R.S.J., 1976. Mechanisms and dynamics of strombolian activity. J. Geol. Soc. London. 132, 429–440.

Burton, M., Allard, P., Muré, F., La Spina, A., 2007. Magmatic gas composition reveals the source depth of slug-driven strombolian explosive activity. Science 317, 227–230.

Chouet, B., 1974. Photoballistics of volcanic jet activity at Stromboli, Italy. J. Geophys. Res. 79, 4961–4976.

Chouet, B., Dawson, P.B., 2010. Seismic source mechanism of degassing bursts at Kilauea Volcano, Hawaii: Results from waveform inversion in the 10–50 s band. J. Geophys. Res. 115, B09311.

Cimarelli, C., Di Traglia, F., Taddeucci, J., 2010. Basaltic scoria textures from a zoned conduit as precursors to violent Strombolian activity. Geology 38, 439–442.

Colò, L., Ripepe, M., Baker, D.R., Polacci, M., 2010. Magma vesiculation and infrasonic activity at Stromboli open conduit volcano. Earth Planet. Sci. Lett. 292, 274–280.

D'Auria, L., Martini, M., 2011. Slug Flow: Modeling in a Conduit and Associated Elastic Radiation, in: Meyers, R.A. (Ed.), Encyclopedia of Complexity and Systems Science. Springer, New York, NY, pp. 858–873.

D'Oriano, C., Bertagnini, A., Pompilio, M., 2010. Ash erupted during normal activity at Stromboli (Aeolian Islands, Italy) raises questions on how the feeding system works. Bull. Volcanol. 73, 471–477.

Del Bello, E., Llewellin, E.W., Taddeucci, J., Scarlato, P., Lane, S.J., 2012. An analytical model for gas overpressure in slug-driven explosions: Insights into Strombolian volcanic eruptions. J. Geophys. Res. 117, B02206.

Gaudin, D., Taddeucci, J., Scarlato, P., Moroni, M., Freda, C., Gaeta, M., Palladino, D.M., 2014. Pyroclast Tracking Velocimetry illuminates bomb ejection and explosion dynamics at Stromboli (Italy) and Yasur (Vanuatu) volcanoes. J. Geophys. Res. Solid Earth 119, 5384–5397.

Gerst, A., Hort, M., Aster, R.C., Johnson, J.B., Kyle, P.R., 2013. The first second of volcanic eruptions from the Erebus volcano lava lake, Antarctica-Energies, pressures, seismology, and infrasound. J. Geophys. Res. Solid Earth 118, 3318–3340.

Gurioli, L., Colo', L., Bollasina, a. J., Harris, a. J.L., Whittington, a., Ripepe, M., 2014. Dynamics of Strombolian explosions: Inferences from field and laboratory studies of erupted bombs from Stromboli volcano. J. Geophys. Res. Solid Earth 119, 319–345.

James, M.., Lane, S.., Chouet, B., Gilbert, J.., 2004. Pressure changes associated with the ascent and bursting of gas slugs in liquid-filled vertical and inclined conduits. J. Volcanol. Geotherm. Res. 129, 61–82.

James, M.R., Lane, S.J., Chouet, B. a., 2006. Gas slug ascent through changes in conduit diameter: Laboratory insights into a volcano-seismic source process in low-viscosity magmas. J. Geophys. Res. 111, B05201.

James, M.R., Lane, S.J., Corder, S.B., 2008. Modelling the rapid near-surface expansion of gas slugs in low-viscosity magmas. Geol. Soc. London, Spec. Publ. 307, 147–167.

James, M.R., Lane, S.J., Wilson, L., Corder, S.B., 2009. Degassing at low magma-viscosity volcanoes: Quantifying the transition between passive bubble-burst and Strombolian eruption. J. Volcanol. Geotherm. Res. 180, 81–88.

Johnson, J.., Lees, J.., 2000. Plugs and chugs—seismic and acoustic observations of degassing explosions at Karymsky, Russia and Sangay, Ecuador. J. Volcanol. Geotherm. Res. 101, 67–82.

Kremers, S., Lavallée, Y., Hanson, J., Hess, K.-U., Chevrel, M.O., Wassermann, J., Dingwell, D.B., 2012. Shallow magma-mingling-driven Strombolian eruptions at Mt. Yasur volcano, Vanuatu. Geophys. Res. Lett. 39, L21304.

Kremers, S., Wassermann, J., Meier, K., Pelties, C., van Driel, M., Vasseur, J., and Hort, M., 2013. Inverting the Source Mechanism of Strombolian Explosions at Mt. Yasur, Vanuatu, using a Multi-Parameter Dataset, J. Volcanol. Geotherm. Res. 262, 104-122.

Kobayashi, T., Namiki, A., and Sumita, I., 2010, Excitation of airwaves caused by bubble bursting in a cylindrical conduit: Experiments and a model, J. Geophys. Res. 115, B10201.

Lane, S.J., James, M.R., Corder, S.B., 2013. Volcano infrasonic signals and magma degassing: First-order experimental insights and application to Stromboli. Earth Planet. Sci. Lett. 377-378, 169–179.

Lautze, N.C., Houghton, B.F., 2005. Physical mingling of magma and complex eruption dynamics in the shallow conduit at Stromboli volcano, Italy. Geology 33, 425.

Lautze, N.C., Houghton, B.F., 2007. Linking variable explosion style and magma textures during 2002 at Stromboli volcano, Italy. Bull. Volcanol. 69, 445–460.

Lighthill, M.J., 1978. Waves in Fluids., Cambridge . ed. Cambridge University Press, Cambridge, UK.

Llewellin, E.W., Del Bello, E., Taddeucci, J., Scarlato, P., Lane, S.J., 2012. The thickness of the falling film of liquid around a Taylor bubble. Proc. R. Soc. A Math. Phys. Eng. Sci. 468, 1041–1064.

Lyons, J.J., Waite, G.P., Ichihara, M., Lees, J.M., 2012. Tilt prior to explosions and the effect of topography on ultra-long-period seismic records at Fuego volcano, Guatemala. Geophys. Res. Lett. 39, n/a–n/a.

McGreger, A.D., Lees, J.M., 2004. Vent discrimination at Stromboli Volcano, Italy. J. Volcanol. Geotherm. Res. 137, 169–185.

Métrich, N., Bertagnini, A., Landi, P., Rosi, M., Belhadj, O., 2005. Triggering mechanism at the origin of paroxysms at Stromboli (Aeolian Archipelago, Italy): The 5 April 2003 eruption. Geophys. Res. Lett. 32, L10305.

Murase, T., McBirney, A., 1973. Properties of some common igneous rocks and their melts at high temperatures. Geol. Soc. Am. Bull. 84, 3563-3592.

Nguyen, C.T., Gonnermann, H. M., Chen, Y., Huber, C., and Maiorano, A. A., 2013, Film Drainage and the Lifetime of Bubbles, Geochem. Geophys. Geosyst. 14, 3616-3631.

O'Brien, G.S., Bean, C.J., Brien, G.S.O., 2008. Seismicity on volcanoes generated by gas slug ascent. Geophys. Res. Lett. 35, L16308.

Parfitt, E. a, 2004. A discussion of the mechanisms of explosive basaltic eruptions. J. Volcanol. Geotherm. Res. 134, 77–107.

Polacci, M., Baker, D.R., Mancini, L., Favretto, S., Hill, R.J., 2009. Vesiculation in magmas from Stromboli and implications for normal Strombolian activity and paroxysmal explosions in basaltic systems. J. Geophys. Res. 114, B01206.

Polacci, M., Corsaro, R.A., Andronico, D., 2006. Coupled textural and compositional characterization of basaltic scoria: Insights into the transition from Strombolian to fire fountain activity at Mount Etna, Italy. Geology 34, 201.

Ruth, D.C.S., Calder, E.S., 2013. Plate tephra: Preserved bubble walls from large slug bursts during violent Strombolian eruptions. Geology 42, 11–14.

Sánchez, C., Álvarez B., Melo F., and Vidal V., 2014, Experimental modeling of infrasound emission from slug bursting on volcanoes, Geophys. Res. Lett. 6705–6711.

Seyfried, R., Freundt, A., 2000. Experiments on conduit flow and eruption behavior of basaltic volcanic eruptions. J. Geophys. Res. 105, 23727.

Taddeucci, J., Pompilio, M., Scarlato, P., 2004. Conduit processes during the July–August 2001 explosive activity of Mt. Etna (Italy): inferences from glass chemistry and crystal size distribution of ash particles. J. Volcanol. Geotherm. Res. 137, 33–54.

Taddeucci, J., Scarlato, P., Capponi, a., Del Bello, E., Cimarelli, C., Palladino, D.M., Kueppers, U., 2012. High-speed imaging of Strombolian explosions: The ejection velocity of pyroclasts. Geophys. Res. Lett. 39, L02301.

Vergniolle, S., Brandeis, G., 1996. Strombolian explosions 1 . A large bubble breaking at the surface of a lava are only slightly damped explosions. J. Geophys. Res. 101, 433–447.

Vergniolle, S., Brandeis, G., J.-C., M., 1996. Strombolian explosions 2. Eruption dynamics determined from acoustic measurements. J. Geophys. Res. 101, 449–466.

Vergniolle, S., Jaupart, C., 1986. Separated two-phase flow and basaltic eruptions. J. Geophys. Res. 91, 12842–12860.

Viana, F., Pardo, R., Yánez, R., Trallero, J.L., Joseph, D.D., 2003. Universal correlation for the rise velocity of long gas bubbles in round pipes. J. Fluid Mech. 494, 379–398.

White, E. T. & Beardmore, R. H., 1962, The velocity of rise of single cylindrical air bubbles through liquids contained in vertical tubes. Chem. Eng. Sci. 17, p. 351–361.

FIGURE AND TABLES WITH CAPTIONS

Table 1. Summary of experimental parameters and scaling to the volcanic case

	Experimental parameters		**Volcanic conditions**		**CFD simulations**	
materials	Water	Castor	Underlying magma	Plug'	Underlying magma	Plug'
Density ρ (kg/m^3)	1000	970	1000		1000	1000
Viscosity μ (Pa s)	0.001	0.986	50	50000	20	20000
Surface tension $\sigma^{\dagger}$ (N/m)	0.07	0.03	0.4	0.4	0.4	0.4
Gravity g (m/s^2)	9.81		9.81		9.81	
Conduit diameter D (m)	0.025		5		3	
Inverse viscosity N_f	12381.68	12.18	700.36	0.70	814.74	0.81
Dimensionless film§ λ'	0.09	0.31	0.14	0.33	0.13	0.33
Film cross section $A^{\#}$	0.16	0.53	0.25	0.55	0.24	0.55
Slug radius r_s (m)	0.01	0.01	2.16	1.68	1.30	1.01
Viscosity contrast μ*	986		1000		1000	
Slug cross section ratio	0.56		0.61		0.60	

§ Calculated from equation 4.2 in Llewellin et al. (2012).
$^{\#}$ Calculated from equation 28 in Del Bello et al. (2012).
† Data for the volcanic case are from Murase and McBirney, 1973.

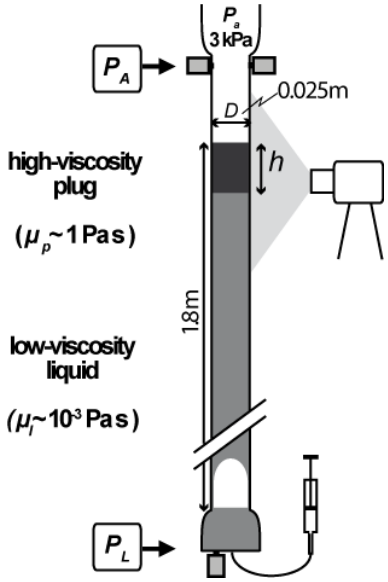

Figure 1. Experimental apparatus. Known volumes of air were injected into the base of a water-filled tube overlain with a high-viscosity 'plug' of thickness *h*. Pressure above the plug was held at 3 kPa. Gas slug ascent, expansion and burst were imaged, and pressure variation was measured in the liquid at tube bottom (ΔP_L) and in air above the free surface (ΔP_A).

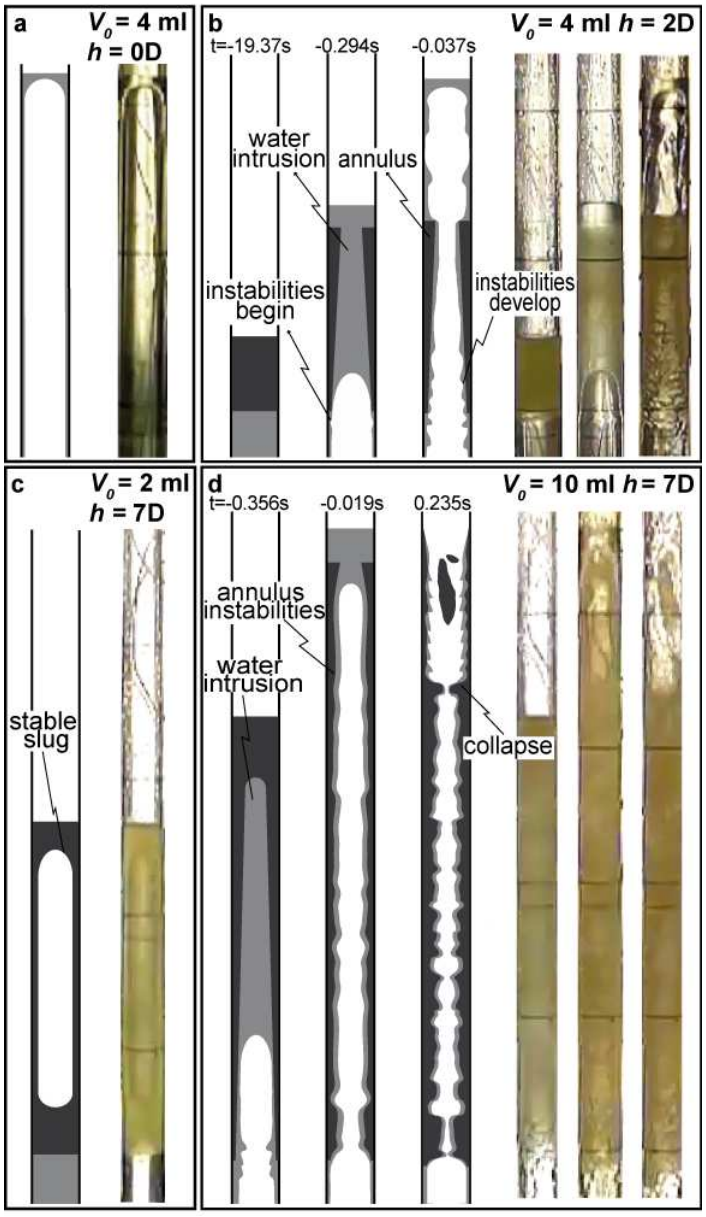

Figure 2. Still frames and interpretive sketches from selected experiments. a) Control experiment without plug (h = 0D) and 4 ml slug. Note smooth slug walls. b) Thin plug experiment (h = 2D). Slug rise and expansion forces water through the plug, forming an oil annulus (-0.294 s relative to burst). The slug rises through the annulus into water extruded above it, and film instabilities develop along the annulus (-0.037 s). c) A thick plug (h = 7D) is deep enough to fully accommodate a 2 ml slug. d) A 10 ml slug rising into the partially water-intruded oil plug causes rippling of the water film (-0.356 s), then its rapid expansion disrupts the upper reaches of the annulus (-0.019). At burst, the oil/water mixture slumps down, hindering or blocking the escaping gas flux (0.235 s).

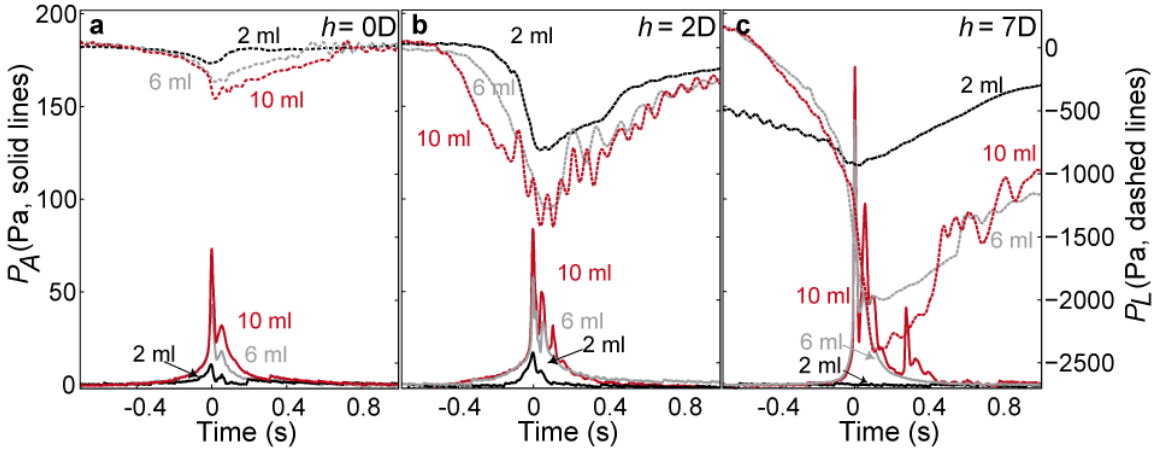

55

56 **Figure 3.** Pressure changes in the liquid at the base of the tube (ΔP_L, dashed lines) and in the air above the free
57 surface (ΔP_A, solid lines), as a function of time and injection gas volume, for a) no plug (h = 0D), b) thin (h = 2D),
58 and c) thick (h = 7D) plug experiments.

59

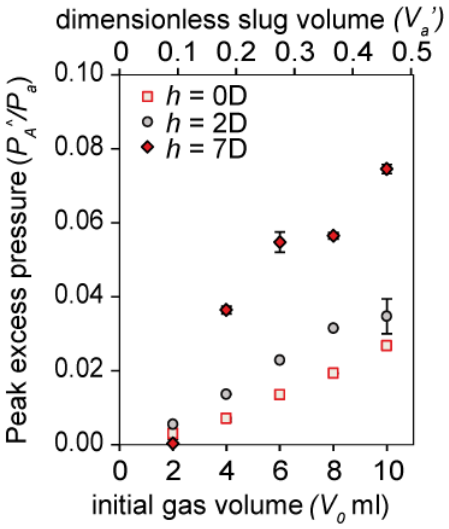

60

61 **Figure 4.** Peak excess pressure $\Delta P_A^{\wedge}$ normalised to P_a is reported as function of volume (V_0). Equivalent V_a' is also
62 reported.

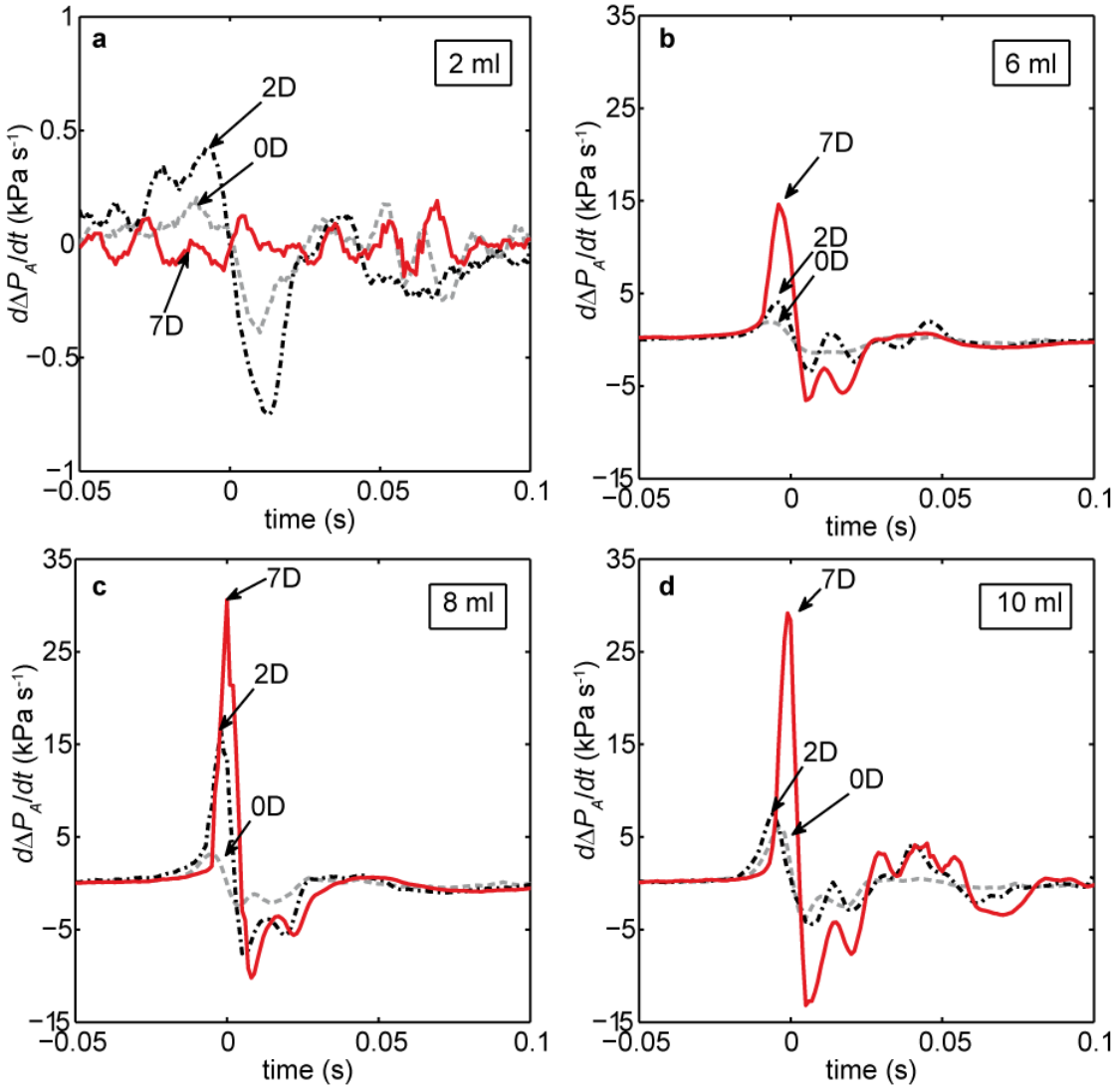

Figure 5. Time derivative of pressure variation $d(\Delta P_A)/dt$ as a function of time for initial air volumes (V_0) of: a) 2 ml ($\boldsymbol{V'_a} = 0.09$), b), 6 ml ($\boldsymbol{V'_a} = 0.28$), c), 8ml ($\boldsymbol{V'_a} = 0.37$), and d) 10 ml ($\boldsymbol{V'_a} = 0.45$) ascending through different plug thicknesses. Such quantities would be equivalent to gas volumes of 7, 22, 29 and 37 m^3 at the volcanic scale, respectively. Note that ~ 80 Hz oscillations emerge on calculation of $d(\Delta P_A)/dt$ and that these plausibly represent high frequency but low amplitude half-wave resonance of gas above the flow in the experimental tube.

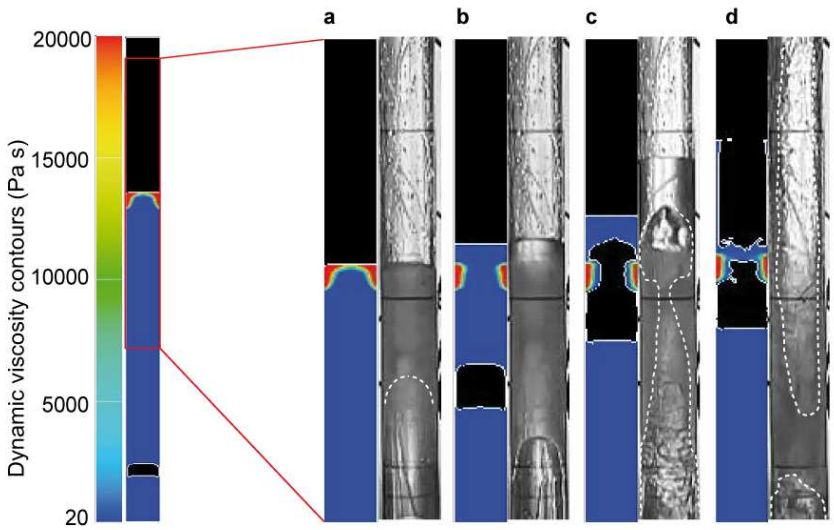

Figure 6. Results from CFD simulation at the volcanic scale. The parameters of the simulation are V_0 = 22 m^3 ($\boldsymbol{V'_a} = 0.28$), P_a = 10^5 Pa, μ_1 = 20 Pas, μ_2 = 20000 Pas; h =6 m (2D), D = 3 m, magma column height 200 m. Still frames (a, b, c, d) extracted from the simulation (see video V05), show good comparison with experiments at the same scaled conditions V_0 = 6 ml ($\boldsymbol{V'_a} = 0.28$) and h =2.5 cm (2D),in terms of burst dynamics and liquid film perturbations, supporting the experimental procedures.

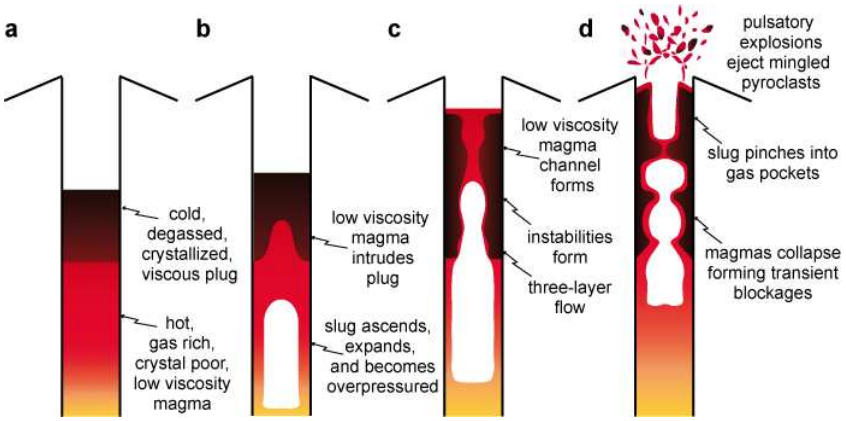

Figure 7 shows a model illustrating the effect of viscous plugging on a strombolian eruption. a) Before slug ascent, degassing and cooling of a magma stagnating atop the conduit forms a high viscosity plug. b) Expansion of the slug, impeded by viscous resistance of the plug, causes low viscosity magma to intrude the plug. c) A three-layer flow forms as the slug enters the low viscosity channel, developing dynamic instabilities. d) Instabilities grow causing mingling of the two magmas, channel collapse, and slug disruption into smaller pockets. Accelerated slug expansion culminates in pulsatory bursting and ejection of mingled pyroclasts. The system then resets to a during the quiescence period before the next slug burst.

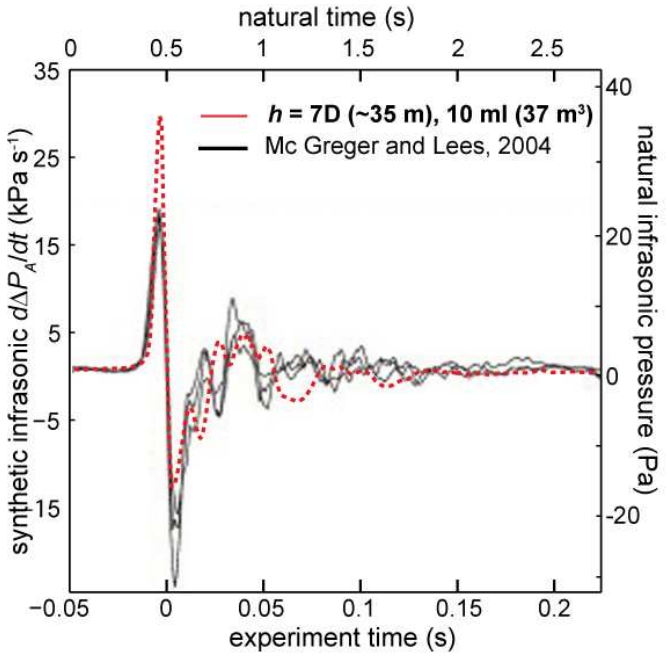

Figure 8. The first time derivative of experimental excess pressure $d(\Delta P_A)/dt$, as a function of time, for the 10 ml, 2D experiment (dashed line) was compared to measured infrasonic signals at Stromboli reprinted from McGreger and Lees (2004 with permission from Elsevier, solid lines). Both time axis and pressure axis are adapted to best fit the experimental to the measured data.

Viscous plugging can enhance and modulate explosivity of strombolian eruptions

E. Del Bello[1], S.J. Lane[2], M.R. James[2], E.W. Llewellin[3], J. Taddeucci[1], P. Scarlato[1], Capponi, A. [2]

[1] *Istituto Nazionale di Geofisica e Vulcanologia, Via di Vigna Murata 605, 00143, Rome, Italy*

[2] *Lancaster Environment Centre, Lancaster University, Lancaster LA1 4YQ, UK*

[3] *Department of Earth Sciences, Durham University, South Road, Durham DH1 3LE, UK*

HIGHLIGHTS

- We present laboratory experiments in which gas slugs ascend a pipe plugged with a viscous liquid
- The presence of a viscous plug enhances burst vigour
- Slug–plug interaction causes pulsatory bursting resembling natural strombolian eruptions
- Experiments indicate slug passage promotes mingling between vertically stratified magmas

Figure1

Click here to download Figure (high-resolution): DelBello_etal_FIG1.eps

Figure2

Click here to download Figure (high-resolution): DelBello_etal_FIG2.eps

Figure 3

Click here to download Figure (high-resolution): DelBelloetal_EPSL-D-15-00041_FIG3.eps

Figure4

Click here to download Figure (high-resolution): DelBello_etal_FIG4.eps

Figure5

Click here to download Figure (high-resolution): DelBello_etal_FIG5.eps

Figure 6

Click here to download Figure (high-resolution): DelBelloetal_EPSL-D-15-00041_FIG6.eps

Figure7

Click here to download Figure (high-resolution): DelBello_etal_FIG7.eps

Figure 8

Click here to download Figure (high-resolution): DelBelloetal_EPSL-D-15-00041_FIG8.eps

Table 1

Click here to download Table: DelBelloetal_EPSL-D-15-00041_TABLE1.xlsx

	Experimental parameters		**Volcanic conditions**		**CFD simulat**
materials	Water	Castor	Underlying magma	Plug'	Underlying magma
Density ρ (kg/m^3)	1000	970	1000		1000
Viscosity μ (Pa s)	0.001	0.986	50	50000	20
Surface tension σ [†] (N/m)	0.07	0.03	0.4	0.4	0.4
Gravity g (m/s^2)	9.81		9.81		9.8
Conduit diameter D (m)	0.025		5		3
Inverse viscosity N_f	12380.68	12.18	700.36	0.70	813.74
Dimensionless film [§] λ'	0.09	0.31	0.14	0.33	0.13
Film cross section A' [#]	0.16	0.53	0.25	0.55	0.24
Slug radius r_s (m)	0.01	0.01	2.16	1.68	1.30
Viscosity contrast μ*	986		1000		10
Slug cross section ratio	0.56		0.61		0.6

[§] Calculated from equation 4.2 in Llewellin et al. (2012).

[#] Calculated from equation 28 in Del Bello et al. (2012).

[†] Data for the volcanic case are from Murase and McBirney, 1973.

Supplementary material for online publication only

Click here to download Supplementary material for online publication only: DelBello_etal_supplementary.docx

Supplementary material (video V01)

Click here to download Supplementary material (video): DelBelloEtAl_V01.mpg

Supplementary material (video V02)

Click here to download Supplementary material (video): DelBelloEtAl_V02.mpg

Supplementary material (video V03)

Click here to download Supplementary material (video): DelBelloEtAl_V03.mpg

Supplementary material (video V04)

Click here to download Supplementary material (video): DelBelloEtAl_V04.mpg

Supplementary material (video V05)

Click here to download Supplementary material (video): DelBelloEtAl_V05.mpg